Expanding the Clinical and Genetic Spectrum of *PCYT2*-related Disorders

Valentina Vélez-Santamaría,[1,2,*] Edgard Verdura,[1,3,*] Colleen Macmurdo,[4] Laura Planas-Serra,[1,3] Agatha Schlüter,[1,3] Josefina Casas,[5] Juan José Martínez,[1,3] Carlos Casasnovas,[1,2,3] Yue Si,[6] Stephanie S.Thompson,[4] Reza Maroofian,[7] Aurora Pujol[1,3,8,*]

[1]Neurometabolic Diseases Laboratory, Bellvitge Biomedical Research Institute (IDIBELL), L'Hospitalet de Llobregat, Barcelona, Spain

[2]Neuromuscular Unit, Neurology Department, Hospital Universitari de Bellvitge, L'Hospitalet de Llobregat, Barcelona, Spain

[3]Centre for Biomedical Research on Rare Diseases (CIBERER), Instituto de Salud Carlos III, Spain.

[4]Division of Medical Genetics, Baylor Scott & White Health, Temple, Texas, USA

[5]RUBAM, Dept Biological Chemistry, IQAC-CSIC; and Liver and Digestive Diseases Networking Biomedical Research Centre (CIBEREHD) ISCIII 28029 Madrid, Spain

[6]GeneDx, Inc., Gaithersburg, Maryland, USA

[7]Genetics Research Centre, Molecular and Clinical Sciences Institute, St. George's University of London, London, United Kingdom

[8]Catalan Institution of Research and Advanced Studies (ICREA), Barcelona, Catalonia, Spain

*contributed equally

Correspondence should be addressed to:

Professor Aurora Pujol, MD, PhD
Neurometabolic Diseases Laboratory, IDIBELL
Hospital Duran i Reynals, Gran Via 199
08908 L'Hospitalet de Llobregat, Barcelona, Spain.
Tel: +34 932607137; Fax: +34 932607414;
Email: apujol@idibell.cat

Short title: Expanding *PCYT2* mutational spectrum

Keywords: PCYT2, hereditary spastic paraplegia

Word count: 1441

Dear Sir,

Recently Vaz *et al.* reported four families with complex hereditary spastic paraplegia (cHSP) and biallelic variants in *PCYT2* encoding CTP:phosphoethanolamine cytidylyltransferase (ET), the rate-limiting enzyme for phosphatidylethanolamine biosynthesis. Patient-derived fibroblasts and plasma had significant abnormalities in both neutral etherlipid and etherphospholipid metabolism (Vaz, McDermott *et al.* 2019). We wish to broaden the phenotypic and genetic spectrum of *PCYT2*-related disorders with two additional patients. Clinical features are detailed in **Table 1**.

Case 1, a 46-year-old man, was born after a normal pregnancy from healthy first cousin consanguineous Spanish parents. He had an older sister who died at the age of 2 years, due to a severe progressive muscle weakness of unknown aetiology. His development was considered as normal during childhood, until 12 years old, when he started to experience frequent falls and difficulties to run and climb. Over the years, he reported weakness and lower limb stiffness. At age 49, neurological examination showed increased tone with proximal symmetrical weakness (MRC 4/5) of the lower limbs. Force and tone were normal in upper limbs. Deep tendon reflexes were globally brisk in all four limbs, with clonus and bilateral extensor plantar responses. He had hypopallesthesia of ankles with no other sensory deficits. No clinical signs of cerebellar involvement were present. He complained of urinary urge incontinence, was treated with baclofen, but improvement in leg spasticity was not clear and urinary urge worsened. Brain MRI at age 46 was strictly normal. Electromyography and nerve conduction studies were largely normal. Currently he is aged 59 years and walks with ankle-foot orthosis braces and needs a walking aid (cane) for large distances. He finished primary school without difficulties, and then he obtained a job as driver. Hitherto, there is no evidence of cognitive impairment.

Case 2 is a 7 years old male born to healthy, nonconsanguineous African American parents. He has two healthy younger sisters. Patient's mother had a positive group B strep test and she was treated with antibiotics prior to delivery. She reported occasional cannabis consumption during pregnancy. Patient was born at 38 weeks and 2 days via spontaneous vaginal delivery, weighting 3.92 kg (44% using CDC charts), with a length of 51 cm (25%), and an occipitofrontal circumference of 35 cm (13%). Apgar scores were 9 at 1 minute and 9 at 5 minutes. He was noted to be tachypneic at 24 hours of life, being admitted to the NICU.

Tachypnea resolved spontaneously and he was discharged home after 26 hours. Ophtalmological assessment at birth showed congenital lateral gaze nystagmus, billateral cataracts and billateral optic atrophy. A global developmental delay was noted very early. He rolled over at 7 months and he did not achieve the ability to sit unsupported, at 3 years he was able to hold a cup. A brain MRI at 7 months was normal, but follow-up MRI at the age of 2.2 years showed an abnormal increased T2/FLAIR signal within the bilateral periventricular white matter, which was consistent with delayed myelination (**Figure 1E**). Epilepsy with multifocal seizures started at 23 months of age. Failure to thrive was noted during infancy, and a gastrostomy tube was placed. Most recent examination, at 7 years of age, shows increased tone in all 4 extremities, globally brisk reflexes and upgoing plantar reflexes bilaterally. His nystagmus improved over time, and he is followed closely for his optic atrophy and cataracts (**Supplemental Figure 1**). He continues with growth restriction, with his weight below 1% on the CDC growth charts with Z-score of -4.17. He has significant intellectual disability/cognitive impairment and attends school in a special education classroom.

Whole exome sequencing (WES) was performed in both patients (methods in **Supplemental Material**). In Case 1 we identified an homozygous missense variant located at the last coding base pair of exon 11, within the donor splice site (NM_001184917.2:c.957G>C,p.(Lys319Asn)) (**Figure 1A, B**). This variant was not carried by his healthy sibling. Copy number (CNV) analysis in patient's WES data excluded the presence of deletions (father's sample was unavailable) (**Supplemental Figure 3**). This variant was absent from gnomAD, strongly conserved, and is located within the second cytidylyltransferase catalytic domain. *In silico* tools predicted an alteration of splicing (Human Splicing Finder and MaxEntScan: -42%). Concordantly, cDNA analysis showed two different transcripts: the first one carried the missense variant, while the second used an alternative donor site in intron 11, resulting in the inclusion of 102 bp into the coding sequence, leading to the insertion of 34 aminoacids (p.(Lys319Asn_Val320ins34)) (**Figure 1C**). This insertion may alter PCYT2 activity by altering active site structure or global PCYT2 protein stability. In Case 2, we identified two compound heterozygous variants: a nonsense variant in exon 11 (NM_001184917.2:c.907delG,p.(Val303Ter)) and a second nonsense in exon 14 resulting into premature truncation of the PCYT2 protein, already reported by Vaz *et al.* in 4 patients (NM_001184917.2:c.1129C>T, p.(Arg377Ter)) (**Supplemental Figure 2**).

To better understand the functional impact of the missense/splicing variant in Case 1, we used lipidomics profiling to quantify the phospholipid content of plasma and peripheral blood mononuclear cells (PBMC). Results showed a phospholipid and glycerolipid dysregulation consistent with previous data from Vaz *et al.* (**Figure 1D**). While most phospholipid species were significantly decreased in Case 1 compared to controls, in particular phosphatidylethanolamine (PE), there was also a significant accumulation of PE[O], as well as the glycerolipids DAG and TAG (diacylglycerol, triacylglycerol). This profile is highly concordant with the lipidomics data reported in Vaz *et al.* 2019, thus providing evidence for an impaired activity of PCYT2 in this patient.

Deleterious variants in *PCYT2* have been proposed by Vaz *et al*. as a new cause of cHSP, defined by HSP combined with global developmental delay, intellectual disability, epilepsy and progressive cerebral atrophy. Our cases broaden the phenotypic and genotypic spectrum with one patient presenting with isolated mild pure HSP, in absence of all additional signs of previously published cases, and a second patient with predominant visual impairment with cataracts, nystagmus, and optic atrophy.

Case 1 shows a pure spastic paraplegia phenotype without any additional signs or abnormal features in a recent brain MRI. The milder disease course may be explained by the phenotypic variability associated to *PCYT2* variants, already reported in Vaz *et al.* For instance, Patient 5, who developed a milder phenotype of cHSP with fine rotary nystagmus and mild intellectual disability, had the same homozygous nonsense variant as Patients 2, 3 and her brother Patient 4, who were more seriously affected. This illustrates the classical phenotypic variability in inborn errors of metabolism (Argmann, Houten et al. 2016). A second explanation concerns the nature of the variant identified. Indeed, the homozygous variant c.957G>C found in Case 1 alters splicing and results into two different transcripts: one containing a missense variant p.(Lys319Asn), and a second one containing in addition, an insertion that probably destabilizes PCYT2 protein. The coexistence of these two transcripts may probably be linked to a less severe effect on PCYT2's activity, although dysregulation of lipidic profiles appeared on the same range.

Although visual impairment was reported in patients 2-5 of the cohort published by Vaz *et al.*, who all harbor the p.(Arg377Ter) allele in homozygosis, only patient 3 was described to have

optic atrophy, thus our Case 2 argues for a higher penetrance of this sign than previously anticipated. Cataracts have only been observed in Case 2 reported in this study, who also harbors a p.(Arg377Ter) allele, and will need to be confirm in additional cases. Intriguingly, through a systems biology approach based in a pairwise correlation with a seed network of *Drosophila melanogaster* genes, *PCYT2* was identified as a candidate gene linked to mouse retinal development (Serb, Orr *et al.* 2010). Moreover, mutations in other genes involved in CDP-choline/CDP-ethanolamine synthesis (Wortmann, Espeel *et al.* 2015) such as *DDHD1* (Bouslam, Benomar *et al.* 2005, Tesson, Nawara *et al.* 2012), *DDHD2* (Schuurs-Hoeijmakers, Geraghty *et al.* 2012, Gonzalez, Nampoothiri *et al.* 2013), *SELENOI* (Ahmed, Al-Khayat *et al.* 2017) and *PNPLA6* (Synofzik, Gonzalez *et al.* 2014) cause both pure and complex HSP combined with eye abnormalities as a common denominator, highlighting the importance of this metabolic pathway in motor neuron and retinal cellular processes (Rickman, Baple *et al.* 2019).

These cases illustrate the utility of WES to establish diagnosis of spastic paraplegias with broad clinical spectrum. This not only ends the diagnostic odyssey, but may even open therapeutic options in the metabolic disorders; for example, choline substitution has already been successfully tested on a *Pcyt2* (+/-) mice with specifically reduced CDP-ethanolamine pathway and metabolic disease (Schenkel, Sivanesan *et al.* 2015). In this animal model choline supplementation improved the lipid profile, restoring fatty acid and triglycerides homeostasis, and therefore assessing its effects on neurological function in human patients would be warranted.

ACKNOWLEDGMENTS

We are indebted to the patients and family members. We thank CERCA Program/Generalitat de Catalunya for institutional support. We also thank Cristina Guilera for her excellent technical assistance.

DATA AVAILABILITY

The data that support the findings of this study are available from the corresponding author, upon reasonable request.

FUNDING

This study was supported by the Centre for Biomedical Research on Rare Diseases (CIBERER) [ACCI14-759], the URDCat program (PERIS SLT002/16/00174), the Hesperia Foundation and the Secretariat for Universities and Research of the Ministry of Business and Knowledge of the Government of Catalonia [2017SGR1206] to AP, and Instituto de Salud Carlos III [PI14/00581] (Co-funded by European Regional Development Fund. ERDF, a way to build Europe) and la Marató de TV3 [345/C/2014] to CC and AP. VV and EV were funded by grants from Instituto de Salud Carlos III (Rio Hortega, CM18/00145; Sara Borrell, CD19/00221). LPS was funded by a predoctoral grant from the Instituto de Salud Carlos III (PFIS, FI18/00141).

COMPETING INTERESTS

Y.S. is an employee of GeneDx, Inc., a wholly owned subsidiary of OPKO Health,Inc. C.M. and S.S.T. are employees of Baylor Scott & White Health. The authors declare that they have no conflict of interest related to the content of this article.

REFERENCES

Ahmed, M. Y., A. Al-Khayat, F. Al-Murshedi, A. Al-Futaisi, B. A. Chioza, J. Pedro Fernandez-Murray, J. E. Self, C. G. Salter, G. V. Harlalka, L. E. Rawlins, S. Al-Zuhaibi, F. Al-Azri, F. Al-Rashdi, A. Cazenave-Gassiot, M. R. Wenk, F. Al-Salmi, M. A. Patton, D. L. Silver, E. L. Baple, C. R. McMaster and A. H. Crosby (2017). "A mutation of EPT1 (SELENOI) underlies a new disorder of Kennedy pathway phospholipid biosynthesis." Brain **140**(3): 547-554.

Argmann, C. A., S. M. Houten, J. Zhu and E. E. Schadt (2016). "A Next Generation Multiscale View of Inborn Errors of Metabolism." Cell Metab **23**(1): 13-26.

Bouslam, N., A. Benomar, H. Azzedine, A. Bouhouche, M. Namekawa, S. Klebe, C. Charon, A. Durr, M. Ruberg, A. Brice, M. Yahyaoui and G. Stevanin (2005). "Mapping of a new form of pure autosomal recessive spastic paraplegia (SPG28)." Ann Neurol **57**(4): 567-571.

Gonzalez, M., S. Nampoothiri, C. Kornblum, A. C. Oteyza, J. Walter, I. Konidari, W. Hulme, F. Speziani, L. Schöls, S. Züchner and R. Schüle (2013). "Mutations in phospholipase DDHD2 cause autosomal recessive hereditary spastic paraplegia (SPG54)." Eur J Hum Genet **21**(11): 1214-1218.

Rickman, O. J., E. L. Baple and A. H. Crosby (2019). "Lipid metabolic pathways converge in motor neuron degenerative diseases." Brain.

Schenkel, L. C., S. Sivanesan, J. Zhang, B. Wuyts, A. Taylor, A. Verbrugghe and M. Bakovic (2015). "Choline supplementation restores substrate balance and alleviates complications of Pcyt2 deficiency." J Nutr Biochem **26**(11): 1221-1234.

Schuurs-Hoeijmakers, J. H., M. T. Geraghty, E. J. Kamsteeg, S. Ben-Salem, S. T. de Bot, B. Nijhof, I. I. van de Vondervoort, M. van der Graaf, A. C. Nobau, I. Otte-Höller, S. Vermeer, A. C. Smith, P. Humphreys, J. Schwartzentruber, B. R. Ali, S. A. Al-Yahyaee, S. Tariq, T. Pramathan, R. Bayoumi, H. P. Kremer, B. P. van de Warrenburg, W. M. van den Akker, C. Gilissen, J. A. Veltman, I. M. Janssen, A. T. Vulto-van Silfhout, S. van der Velde-Visser, D. J. Lefeber, A. Diekstra, C. E. Erasmus, M. A. Willemsen, L. E. Vissers, M. Lammens, H. van Bokhoven, H. G. Brunner, R. A. Wevers, A. Schenck, L. Al-Gazali, B. B. de Vries, A. P. de Brouwer and F. C. Consortium (2012). "Mutations in DDHD2, encoding an intracellular phospholipase A(1), cause a recessive form of complex hereditary spastic paraplegia." Am J Hum Genet **91**(6): 1073-1081.

Serb, J. M., M. C. Orr and M. H. West Greenlee (2010). "Using evolutionary conserved modules in gene networks as a strategy to leverage high throughput gene expression queries." PLoS One **5**(9).

Synofzik, M., M. A. Gonzalez, C. M. Lourenco, M. Coutelier, T. B. Haack, A. Rebelo, D. Hannequin, T. M. Strom, H. Prokisch, C. Kernstock, A. Durr, L. Schöls, M. M. Lima-Martínez, A. Farooq, R. Schüle, G. Stevanin, W. Marques and S. Züchner (2014). "PNPLA6 mutations cause Boucher-Neuhauser and Gordon Holmes syndromes as part of a broad neurodegenerative spectrum." Brain **137**(Pt 1): 69-77.

Tesson, C., M. Nawara, M. A. Salih, R. Rossignol, M. S. Zaki, M. Al Balwi, R. Schule, C. Mignot, E. Obre, A. Bouhouche, F. M. Santorelli, C. M. Durand, A. C. Oteyza, K. H. El-Hachimi, A. Al Drees, N. Bouslam, F. Lamari, S. A. Elmalik, M. M. Kabiraj, M. Z. Seidahmed, T. Esteves, M. Gaussen, M. L. Monin, G. Gyapay, D. Lechner, M. Gonzalez, C. Depienne, F. Mochel, J. Lavie, L. Schols, D. Lacombe, M. Yahyaoui, I. Al Abdulkareem, S. Zuchner, A. Yamashita, A. Benomar, C. Goizet, A. Durr, J. G. Gleeson, F. Darios, A. Brice and G. Stevanin (2012). "Alteration of fatty-acid-metabolizing enzymes affects mitochondrial form and function in hereditary spastic paraplegia." Am J Hum Genet **91**(6): 1051-1064.

Vaz, F. M., J. H. McDermott, M. Alders, S. B. Wortmann, S. Kölker, M. L. Pras-Raves, M. A. T. Vervaart, H. van Lenthe, A. C. M. Luyf, H. L. Elfrink, K. Metcalfe, S. Cuvertino, P. E. Clayton, R. Yarwood, M. P. Lowe, S. Lovell, R. C. Rogers, A. H. C. van Kampen, J. P. N. Ruiter, R. J. A. Wanders, S. Ferdinandusse, M. van Weeghel, M. Engelen, S. Banka and D. D. D. Study (2019). "Mutations in PCYT2 disrupt etherlipid biosynthesis and cause a complex hereditary spastic paraplegia." Brain **142**(11): 3382-3397.

Wortmann, S. B., M. Espeel, L. Almeida, A. Reimer, D. Bosboom, F. Roels, A. P. de Brouwer and R. A. Wevers (2015). "Inborn errors of metabolism in the biosynthesis and remodelling of phospholipids." J Inherit Metab Dis **38**(1): 99-110.

LEGENDS

Figure 1: Family trees and *PCYT2* mutation features.

A) Family trees. Square: male, circle: female, black symbols: affected individuals, white symbols: unaffected carriers, WT: wild-type allele. Double line indicates consanguinity.

B) Gene structure of *PCYT2* and reported mutations. Blue boxes represent *PCYT2* exons. Mutations in italics (above) represent mutations reported by Vaz *et al*., 2019, and mutations in bold (below) represent variants identified in this paper. Amino acid sequence alignments of *PCYT2* across several species demonstrate conservation of the residues mutated by missense variants.

C) cDNA analysis of PCYT2 in Cases 1. Left, agarose gel electrophoresis showing the presence of two transcript in Case 1. Right, Sanger sequence analysis of isolated bands from agarose gels.

D) Lipid profile in human plasma and PBMC. CTL (n=5) and Case 1 (n=1). Data represented as mean ± SD (relative pmolequiv/ml in plasma and pmol eq/mg protein in PBMC) shown as fold increase of the patient compared to that of control individuals, who were sex and age-matched. **P<0,05, **P<0,01, ***P<0,001* (2-tailed Student's *t*-test). PE: phosphatidylethanolamine. PC: phosphatidylcholine. PS: Phosphatidylserine. PE[O], PC[O]: phosphatidylethanolamine and phosphatidylcholine etherphospholipids. LPE and LPC: lysophosphatidylethanolamine and lysophosphatidylcholine. DAG, TAG: diacylglycerol, triacylglycerol.

E) Brain MRI sequences of Case 2. Axial (left) and sagital (right) fluid-attenuated inversion recovery (FLAIR) shows increased signal within the bilateral periventricular white matter, consistent with delayed myelination.

	Case 1	Case 2	Vaz *et al.*, 2019 (Patients 1, 2, 3, 4, 5 respectively)
General information			
Age at last assessment (years)	59	5	5.8, 20, 16.7, 9.9, 2.5
Gender	Male	Male	Male, Male, Male, Female, Male
Ethnicity	Spanish	African American	Hungarian, British, Turkish, US Caucasian, US Caucasian
Examination			
Dysmorphic features	No	High columella insertion with long appearing philtrum, broad nasal root, high arched palate	None of them
Spasticity	Yes	Yes, spastic quadriparesis	All patients
Hyperreflexia	Yes	Yes	All patients
Extensor Plantar Response	Yes	Yes	All patients
Other neurological features			
Developmental delay	No	Yes	All patients, ranging from mild to severe
Intellectual disability	No	Yes	All patients, ranging from mild to severe
Epileptic seizures	No	Multifocal epilepsy	All patients
Cerebellar ataxia	No	Yes	Patient 2
Hearing loss	No	No	Patient 3
Ophthalmological symptoms			
Cataracts	No	Yes, congenital cataracts	Not reported
Nystagmus	No	Yes, congenital nystagmus	Patients 2,3,4 and 5
Optic atrophy	No	Yes	Patient 3
Investigations			
Brain MRI	Normal	Abnormal increased T2/FLAIR signal within the bilateral periventricular white matter	Patients 1,2,3 and 4: Progressive atrophy with subtle symmetric hyperintensities in the cerebral white matter (Patient 5 not performed)

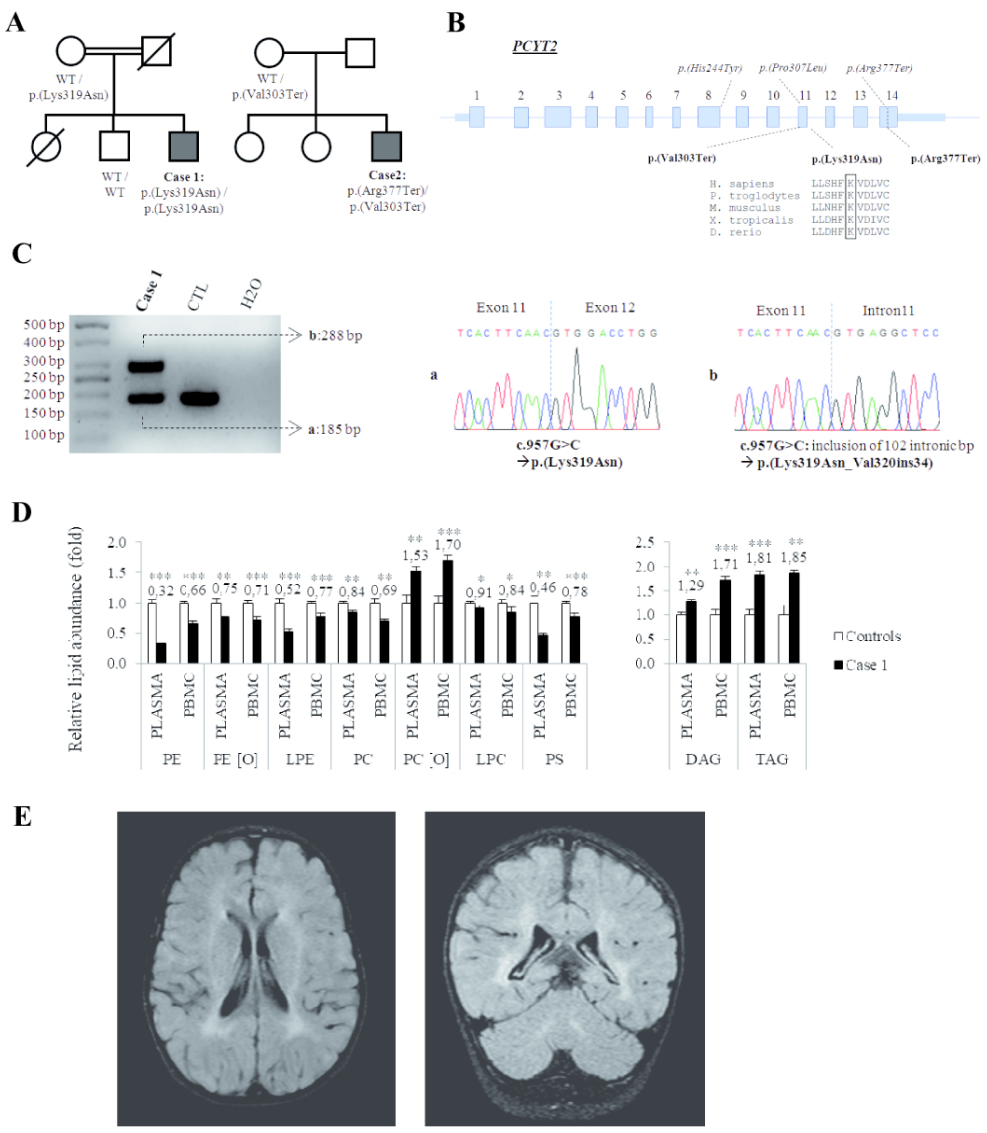

Figure 1: Family trees and PCYT2 mutation features. A) Family trees. Square: male, circle: female, black symbols: affected individuals, white symbols: unaffected carriers, WT: wild-type allele. Double line indicates consanguinity. B) Gene structure of PCYT2 and reported mutations. Blue boxes represent PCYT2 exons. Mutations in italics (above) represent mutations reported by Vaz et al., 2019, and mutations in bold (below) represent variants identified in this paper. Amino acid sequence alignments of PCYT2 across several species demonstrate conservation of the residues mutated by missense variants. C) cDNA analysis of PCYT2 in Cases 1. Left, agarose gel electrophoresis showing the presence of two transcript in Case 1. Right, Sanger sequence analysis of isolated bands from agarose gels. D) Lipid profile in human plasma and PBMC. CTL (n=5) and Case 1 (n=1). Data represented as mean ± SD (relative pmolequiv/ml in plasma and pmol eq/mg protein in PBMC) shown as fold increase of the patient compared to that of control individuals, who were sex and age-matched. *P<0,05, **P<0,01, ***P<0,001 (2-tailed Student's t-test). PE: phosphatidylethanolamine. PC: phosphatidylcholine. PS: Phosphatidylserine. PE[O], PC[O]: phosphatidylethanolamine and phosphatidylcholine etherphospholipids. LPE and LPC: lysophosphatidylethanolamine and lysophosphatidylcholine. DAG, TAG: diacylglycerol, triacylglycerol. E) Brain MRI sequences of Case 2. Axial (left) and sagital (right) fluid-attenuated inversion recovery (FLAIR) shows increased signal within the bilateral periventricular white matter, consistent with delayed myelination.

90x104mm (300 x 300 DPI)

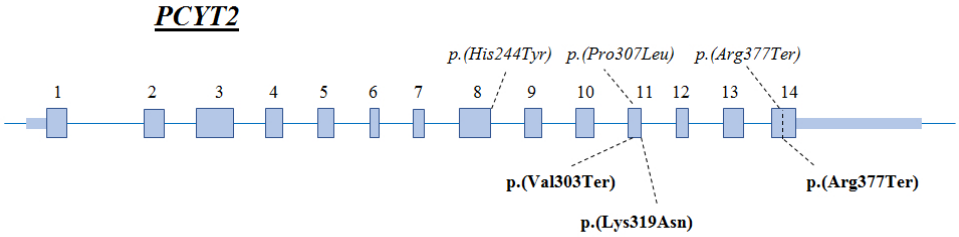

262x80mm (96 x 96 DPI)

SUPPLEMENTARY METHODS

1. Clinical evaluation
2. Whole exome sequencing
3. RNA splicing analysis
4. Lipidomic analysis
5. Statistical analysis

Clinical evaluation

Patients gave written informed consent according to the Declaration of Helsinki for the collection and storage of clinical data, blood samples and publication. The study was approved by the local ethics committees.Detailed neurological examinations were performed on all members of the family. Blood samples and skin-derived fibroblast cell lines were obtained using standard methods.

Whole exome sequencing

Whole Exome Sequencing was carried out using the SeqCap Exome V3.0 64Mb kit (Nimblegen) and sequenced with 100-bp paired-end reads, generated on a HiSeq2000 Platform (Illumina, Inc. USA). Sequencing and variant analysis protocols followed the Genome Analysis Tool Kit (GATK) pipeline (McKenna, Hanna *et al*., 2010). Variant prioritization was based on an autosomal recessive pattern of inheritance (MAF <0.1%). Initial analysis of WES data did not lead to a diagnosis. Reanalysis after publication of Vaz*et al.*, was performed in combination with in-house phenotype-driven methods that rank the variants related to the patient's phenotype. *PCYT2* variants were confirmed via Sanger sequencing (primers available upon request).

RNA splicing analysis

Fibroblast cell lines from Case 1and controls were cultured at 37°C and 5% CO2 in Dulbecco's modified eagle medium (DMEM) supplemented with 10% fetal bovine serum (FBS) and 100U/ml penicillin + 100µl/ml streptomycin. RNA was extracted using the RNeasy Mini Kit (QIAGEN) and cDNA was synthesized using the

Superscript IV kit (Life Technologies) following manufacturer's instructions. cDNA was amplified by polymerase chain reaction (PCR) using primers targeting *PCYT2* exons followed by gel electrophoresis (3%), amplicon purification and Sanger sequencing.

185 bp

F: TGAATCTGCATGAACGGACT (exon 10)
R: TCTCTTGGGCTCCTGGTATG (exon 13)

Lipidomics analysis

Whole blood was centrifuged at 400xg for 30 min using a gradient of Histopaque(Sigma-Aldrich) to separate plasma, erythrocytes and peripheral blood mononuclear cells (PBMC) for Case 1. PBMC protein concentration was determined by BCA protein assay kit (Thermo Fisher Scientific). Lipids were analyzed as described [1, 2] with minor modifications. In detail, for phospholipids and neutral lipids a total of 750µl of a methanol-chloroform (1:2, vol/vol) solution containing internal standards (16:0 D31_18:1 phosphocholine, 16:0 D31_18:1 phosphoethanolamine, 16:0 D31-18:1 phosphoserine, 17:0 lyso-phosphocholine, 17:1 lyso-phosphoethanolamine, 17:1 lyso-phosphoserine, 17:0 D5_17:0 diacylglycerol, 17:0/17:0/17:0 triacylglycerol and C17:0 choresteryl ester, 0.2nmol each, from Avanti Polar Lipids) were added to 0.002ml plasma of 0.2mg protein of PBMC lysate.Samples were vortexed and sonicated until they appeared dispersed and extracted at 48ºC overnight. The samples were then evaporated and transferred to 1.5ml Eppendorf tubes after the addition of 0.5ml of methanol and let to evaporate to dryness. Before analysis, 150µl of methanol were added to the samples, centrifuged at 13000xg for 3 min, and 130µl of the supernatants were transferred to ultra-performance liquid chromatography (UPLC) vials for injection and analysis.

All lipidswere analyzed by liquid chromatography-high resolution mass spectrometry (LC-HRMS) using an Aqcuity ultra high-performance liquid chromatography (UHPLC) system (Waters, USA) connected to a Time of Flight (LCT Premier XE) Detector. Full scan spectra from 50 to 1800Da were acquired, and individual spectra were summed to

produce data points each of 0.2sec. Mass accuracy at a resolving power of 10000 and reproducibility were maintained by using an independent reference spray via the LockSpray interference. Lipid extracts were injected onto an Acquity UHPLC BEH C8 column (1.7µm particle size, 100mm x 2.1mm, Waters, Ireland) at a flow rate of 0.3ml/min and a column temperature of 30ºC. The mobile phases were methanol with 2mM ammonium formate and 0.2% formic acid (A)/water with 2mM ammonium formate and 0.2% formic acid (B).

Positive identification of compounds was based on the accurate mass measurement with an error B5 ppm and its LC retention time, compared with that of a standard (92%).Quantification was carried out using the extractedion chromatogram of each compound, using 50mDa windows. The linear dynamic range was determined by injecting mixtures of internal and natural standards as indicated above. Since standards for all identified lipids were not available, the amounts of lipids are given as pmol equivalents relative to each specific standard.

Five plasma and PBMC samples from healthy individuals were used as controls. Two replicates were extracted for Case 2 samples.

Statistical analysis

Statistical significance was assessed using Student's *t*-test whenever two groups were compared and was considered meaningful at p-value < 0,05.

REFERENCES:

1. Simbari F, McCaskill J, Coakley G, Millar M, Maizels RM, Fabriás G, Casas J, Buck AH. Plasmalogen enrichment in exosomes secreted by a nematode parasite versus those derived from its mouse host: implications for exosome stability and biology. *Journal of Extracellular Vesicles***2016**, 5: 30741

2. Barbacini P, Casas J, Torretta E, Capitanio D, Maccallini G, HirschlerV, Gelfi C. Regulation of serum sphingolipids in Andean Children born and living at high altitude (3775 m). *Int J MolSci*, **2019**, *20*(11), 2835

Supplemental Table 1:Patients' variant frequency.

Hg19	**cDNA** (NM_001184917.2)	**Protein**	**gnomAD frequency**
Chr17:79862804G>A	c.(1129C>T)	p.(Arg377Ter)	16 heterozygous carriers (279.032 alleles)
Chr17:79863546C>G	c.(957G>C)	p.(Lys319Asn)	Absent (250.856 alleles)
Chr17:79863596delC	c.(907delG)	p.(Val303Ter)	1 heterozygous carrier (31.312 alleles)

Supplemental Figure 1: Photographs of Case 2's eyes, showing congenital cataracts. A. Left eye B. Right eye.

A **B**

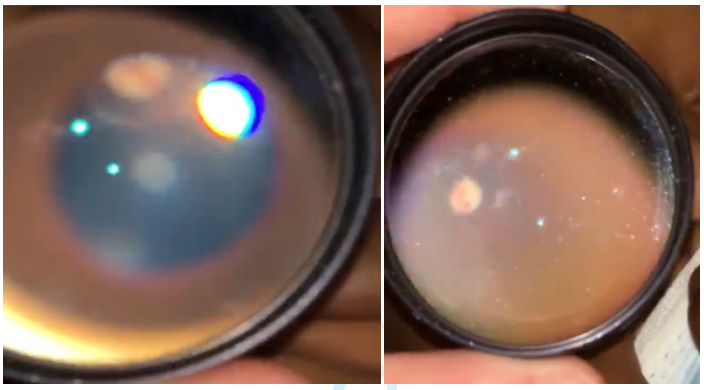

Supplemental Figure 2: Sanger sequencing results.

Case 1

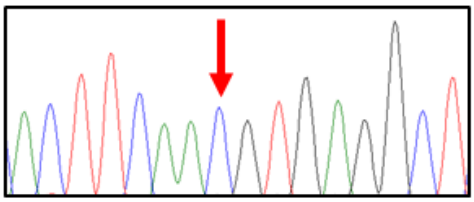

c.957G>C, p.(Lys319Asn)

Case 2

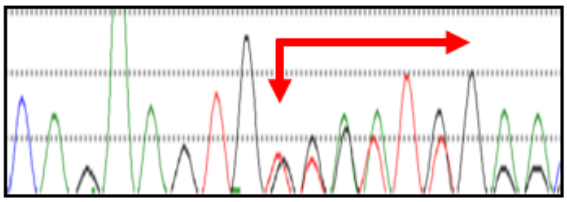

c.907delG, p.(Val303Ter)

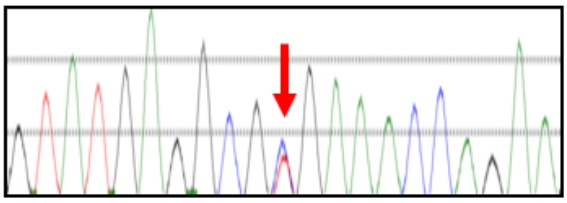

c.1129 C>T, p.(Arg377Ter)

Supplemental Figure 3: Lack of deletions in Case 2's *PCYT2* region. Above: IGV screenshot of *PCYT2* region in Case 2's .bam file. Below: local coverage of *PCYT2* (Case 2 and a healthy control).

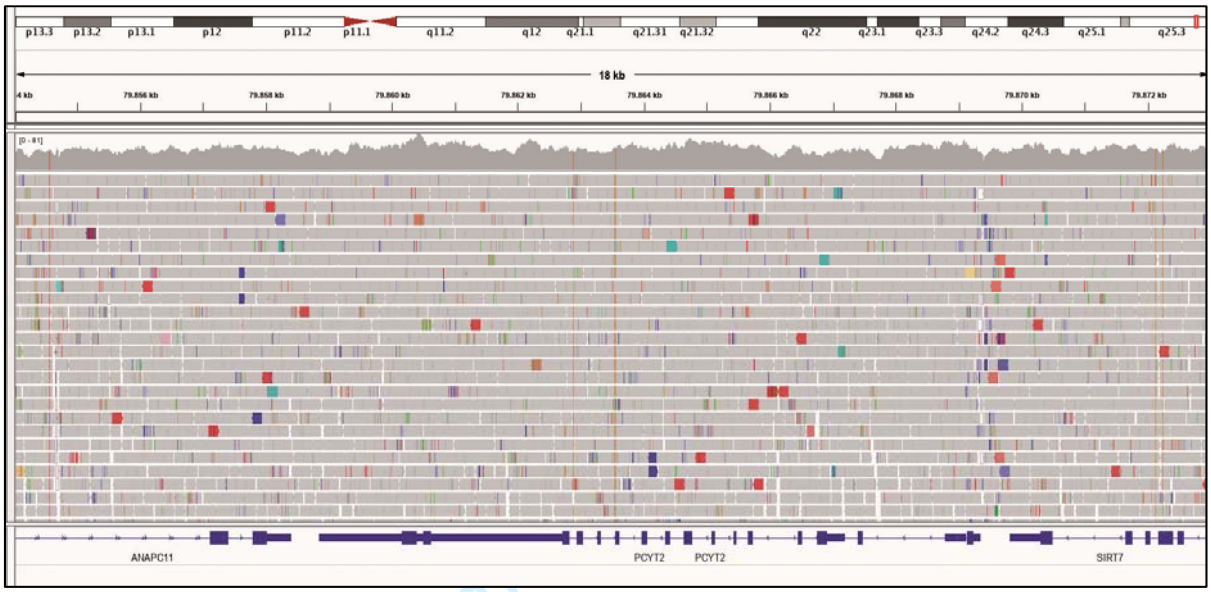

PCYT2 → chr17:79.858.834-79.869.275